Self-Assembly of Conjugated Polymers and ds-Oligonucleotides Directed Fractal-like Aggregates

Haiyang Gan,[†,‡] Yuliang Li,*[,†] Huibiao Liu,[†] Shu Wang,[†] Cuihong Li,[†,‡] Mingjian Yuan,[†,‡] Xiaofeng Liu,[†,‡] Chunru Wang,[†] Lei Jiang,[†] and Daoben Zhu[†]

Beijing National Laboratory for Molecular Sciences (BNLMS), CAS Key Laboratory of Organic Solids, Institute of Chemistry, and Graduate School of Chinese Academy of Sciences, Chinese Academy of Sciences, Beijing 100080, People's Republic of China

Received January 22, 2007; Revised Manuscript Received March 11, 2007

Highly ordered nanostructures between conjugated polymers and ds-oligonucleotides have been first fabricated by simply controlling the self-assembly processes, which shows a novel concept for fabricating fractal-like structures. The formation of polymer/DNA fractal-like aggregates is a diffusion-limited aggregation (DLA) process. The fractal dimension is independent of the polymer/DNA concentration but only related to the polymer/DNA charge ratio. More interestingly, the different fluorescent resonance energy transfer (FRET) behavior between the polymer and the DNA can be used to distinguish dsDNA from ssDNA.

Introduction

The design and synthesis of functionalized nanostructures with controlled dimensions remain a challenging and attractive target of both biology and the nanosciences.[1,2] As a means of creating designed nanomaterials, molecular self-assembly has attracted considerable attention. Like organic building blocks, the sophisticated biological macromolecules, such as polysaccharides, peptides, and proteins, have also been used to produce ordered nanostructures.[3−6] DNA is a semiflexible, highly negatively charged polyelectrolyte that can fold into tightly packed toroidal condensates in the presence of cationic polyamines or cationic surfactants.[7,8] Recently, the aggregation of these DNA−polycation condensates has also been investigated.[9,10] However, highly ordered fractal aggregates of DNA−polymer have seldom been reported.[11] The diversity of geometrical fractal molecular motifs, such as 2D and 3D assemblies, is considered as essential elements in biocomputation devices.[12] In this point of view, the research of using cationic polymers to condense DNA into nanoscale complexes accompanied subsequently by self-assembly would be of great interest in both fundamental and practical fields.[13]

Conjugated polymers have established themselves as useful materials in optoelectronic applications.[14,15] Their electrical and optical properties can be controlled by molecular conformations and supramolecular assembly.[16−19] In this aspect, various low-dimension morphologies, such as spherical nanoparticles, nanowires, and nanotubes,[19,20] have been fabricated. However, the challenges still remain in the fabrication of new conjugated polymer materials with well-defined and highly ordered nanostructures.

In this paper, we examined whether the highly ordered nanostructures can be fabricated by simply controlling the self-assembly process. Herein we would like to report a novel concept for fabricating fractal-like aggregates of cationic conjugated polymers by self-assembly with oligonucleotides. The oligo-dsDNA labeled with a fluorescein at the 5′-terminus (dsDNA-fl, the sequence is 5′-Fl-ATCTTGACTATGTGGGT-GCTAACTC-3′, corresponding to the mus musculus chromosome 1, Genbank accession number AC124821.5) and two kinds of polyphenyleneethynylene (PPE) (for the structures of the polymers see Scheme 1) are anionic and cationic moieties, respectively. We chose these two PPEs because they are easy to synthesize and have a different shape of backbone.[21,22] Among the used PPEs, PPE2 with *m*-phenylene units has more conformational freedom, in comparison to linear PPE1 with a linear backbone structure. The conformational freedom could make PPE2 more easily adapt to the range of secondary structures presented by DNA macromolecules. More interestingly, it was found that the different fluorescence resonance energy transfer (FRET) behavior between PPEs and DNAs could be used to distinguish dsDNA from ssDNA.

Experimental Section

Materials. The oligonucleotides were purchased from Shanghai Sangon Biological Engineering Technology and Service Co. Ltd. The synthesis of the cationic PPEs began with the polymerization of the monomers in the presence of palladium catalyst (Sonogashira−Hagihara coupling), followed by quaternization with ethyl iodide.

The synthetic route for the polymers is shown in Scheme 2. All chemical reagents used were purchased from Acros Chemical Company and Beijing Chemical Reagent Company. The detailed synthetic procedure of the monomer can be found anywhere.[23]

Polymerization. For the general polymerization process, under argon protection, diisopropylamine/toluene (3:7, 15 mL) (for polymerization of PPE1, we use diisopropylamine/$CHCl_3$ 3:7) was added to a 25 mL round-bottom flask containing a 0.140 g (0.39 mmol) sample of 1,4-diethynylbenzene (or 1,3- diethynylbenzene), 0.210 g of diiodobenze monomer (0.38 mmol), 26 mg (0.024 mmol) of $Pd(PPh_3)_4$, and 21 mg (0.11 mmol) of CuI. The mixture was heated at 70 °C for 24 h and then subjected to a $CHCl_3/H_2O$ solvent mixture. The combined organic phase was washed with ammonia water (50%) twice, water twice, and brine once, and dried over $MgSO_4$. The solution was removed in vacuum, and the residue was redissolved in 10 mL of $CHCl_3$ and reprecipitated in methanol twice. The mixture was filtered to afford a yellow solid (yield 76−84%). The gel permeation chromatography

* Corresponding author. Phone: +86-10-62588934. Fax: +86-10-82616576. E-mail: ylli@iccas.ac.cn.

† Institute of Chemistry.

‡ Graduate School of Chinese Academy of Sciences.

10.1021/bm070082k CCC: $37.00
Published on Web 04/26/2007

Scheme 1

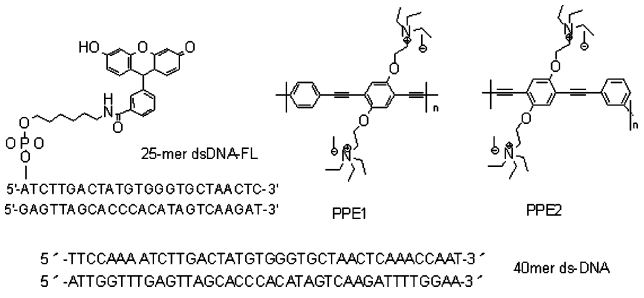

(GPC) experiment shows that the molecular weight M_n of PPE1 and PPE2 is 1.5×10^4 and 9.6×10^3, respectively.

Quaternization. In a 25 mL round-bottom flask 0.5 mmol (based on repeat unit) of neutral polymer was added. The polymer was dissolved in 10 mL of tetrahydrofuran. To this was added ethyl iodide (0.78 g, 5 mmol) and 5 mL of dimethyl sulfoxide. The solution was stirred at 50 °C for 24 h. During the quaternization, a yellow precipitate was produced in the solution. The resulting precipitate was collected by centrifugation, washed with tetrahydrofuran and dried to get the desired product, yield 98%.

Characterization. All measurements were recorded in aqueous solutions. Circular dichroism (CD) spectra were recorded on a JASCO J-810 CD spectrophotometer with the data pitch of 0.1 nm at room temperature. In a typical experiment, 200 μL of DNA solution (5×10^{-6} M) was transferred to quartz cell and titrated with PPE solution at a concentration (each time 20 μL was added) of 4×10^{-4} M. The FRET experiments were carried out on a Hitachi F-4500 spectrometer, using 90° angle detection for solution samples.

Field emission scanning electron microscopy (FESEM) images were taken on a JSM 6700F NT instrument. The silicon wafer was carefully washed and hydrophilized by treatment with H_2SO_4 and H_2O_2 solution (volume ratio 7:3) at 50 °C for 1 h before use. The polymer/DNA complexes solutions were applied onto the silicon wafers and dried under ambient conditions. To extend the assembly time, the deposited silicon wafers were put in a moisture atmosphere and dried slowly. (In ambient atmosphere it usually takes 10−20 min to dry.)

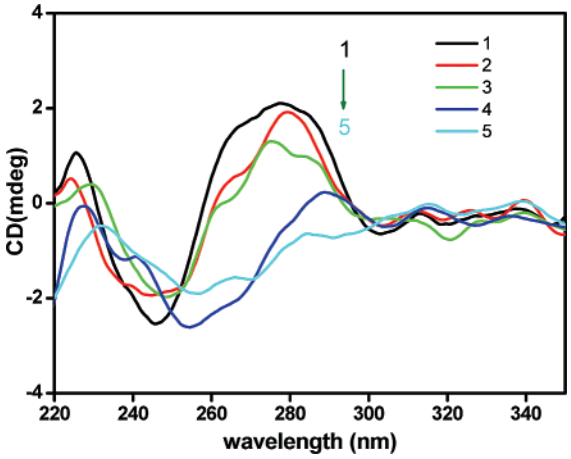

Figure 1. CD spectra of 5×10^{-6} M DNA with different concentrations of PPE1; from curve 1 to curve 5 the PPE1/DNA ratios are 0, 0.2, 0.4, 0.6, and 0.8 in water.

The optical image and confocal laser scanning microscopy images were detected on a scanning near-field optical microscope (Witec Alpha SNOM). The fluorescence from the sample was collected using a Melles Griot He−Cd laser (442 nm) as the excitation source. The emission of 488−588 nm of the sample was detected and imaged.

Results and Discussion

When PPEs and DNA were mixed, they formed PPE/DNA interpolyelectrolyte complexes, which were confirmed by the emission and CD spectra of PPE and PPE/DNA complexes. Both the two PPEs have efficient FRET from the polymers to dsDNA-fl. The detailed FRET experiments will be discussed later. The CD spectra can be used to monitor the conformational transition of dsDNA. In this case, PPE1 and PPE2 gave similar results. In the absence of PPE, the CD spectrum of oligo-dsDNA was a typical B-form, which exhibited a positive Cotton effect

Scheme 2

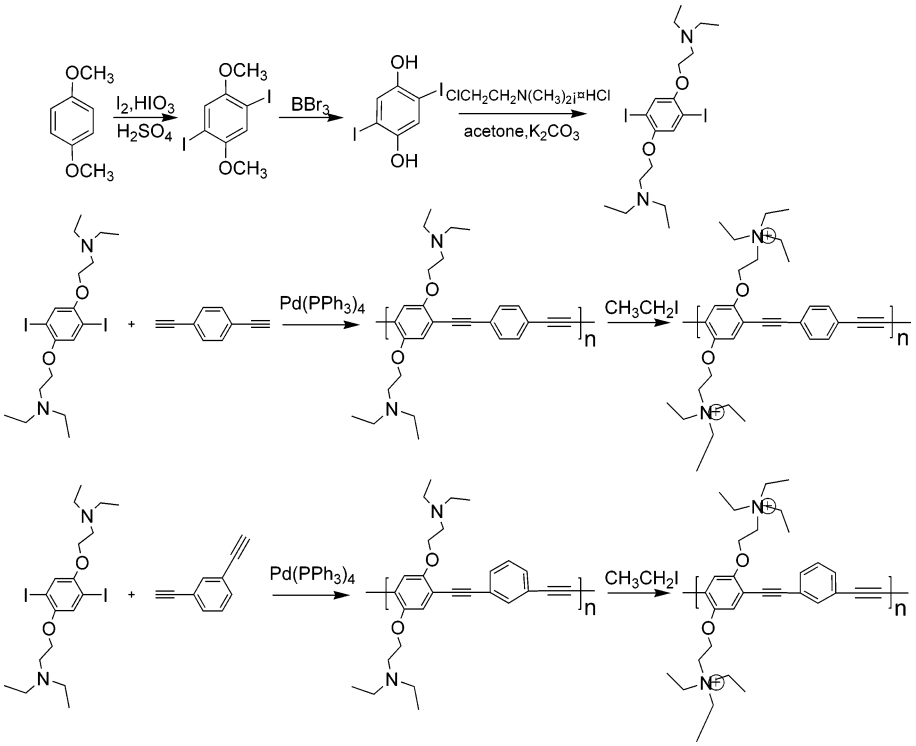

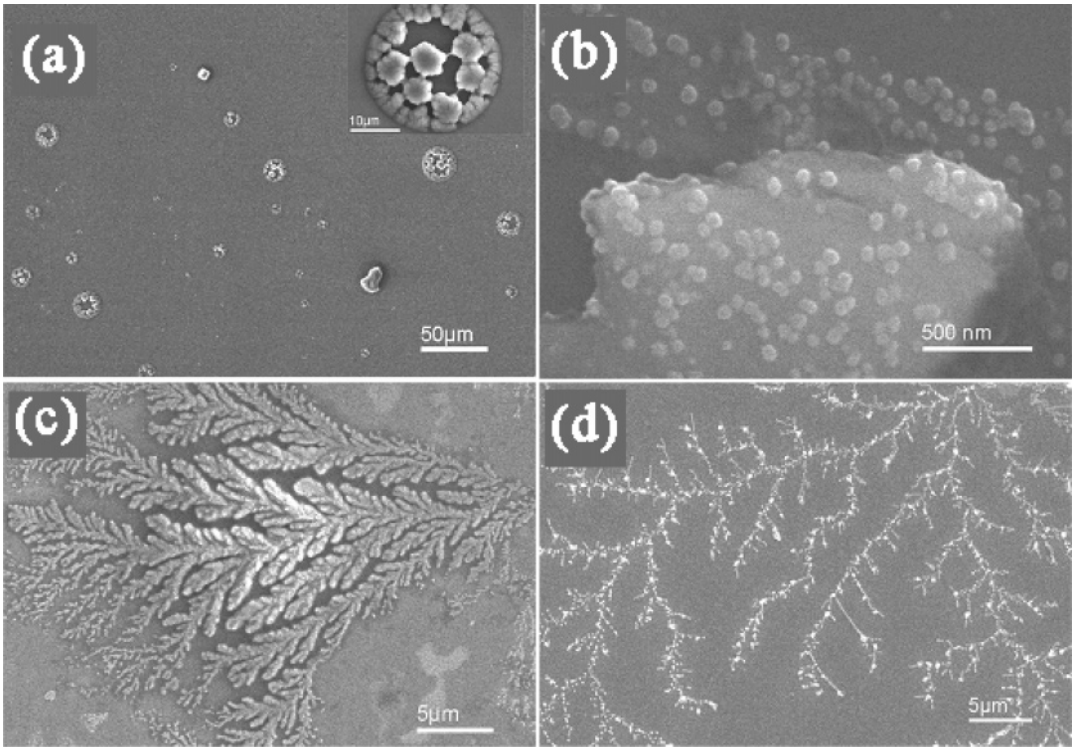

Figure 2. SEM images of (a) dsDNA with the concentration of 5×10^{-7} M; (b) PPE1 with the concentration of 5×10^{-5} M (PPE2 give similar images); (c) PPE1/dsDNA complexes with the DNA concentration of 1×10^{-7} M and PPE1/DNA charge ratio of 1:4; (d) fractal-like structure of PPE1/dsDNA complexes with the DNA concentration of 1×10^{-7} M and PPE1/dsDNA charge ratio of 1:1.

at 276 nm and a negative one at 246 nm, as shown in Figure 1. When the PPE/dsDNA charge ratio was low, the CD peaks were slightly reduced. When the PPE was added continuously, the height of the positive peak decreased gradually, accompanied with a red shift of both the positive and the negative peaks, indicating a transition of the secondary dsDNA structure from the B- to C-form.[24] The change in the intensity of the CD peak at 278 nm was associated with the alteration of hydration of the helix in the vicinity of phosphate or ionic concentrations of the ribose ring.[25] We therefore suggest that replacement of sodium ion by the PPEs backbone could result in a change in the hydration near the phosphate group of the DNA helix since the polymer backbone is hydrophobic. The CD experiment proved that the conformational transition of DNA occurred at the higher PPE/DNA charge ratio, for example, near 1:1.

The oligo-dsDNA molecules formed particles on the silicon substrate, as shown in Figure 2a. Figure 2b shows that the cationic polymers on the silicon substrate cast from aqueous solution formed nanoparticle aggregates. When the oligo-dsDNA solution was added to cationic polymers, they assembled spontaneously through electrostatic interactions and resulted in fractal-like condensed interpolyelectrolyte complexes, as shown in Figure 2c. (Similar images were obtained when we used PPE2.)

The fractal dimension was measured using the divider formula $\mathrm{Df} = \lim(r \rightarrow 0)[\log N(r)/\log(r)]$, where r is the length unit, $N(r)$ is the size of the geometric object measured with the unit r. The detailed procedure can be found in previous literatures.[26] The graph of $\log(r)$ versus $\log N(r)$ followed a straight line. The absolute value of the slope gave the fractal dimension Df $= 1.70$. Figure 2d shows fractal-like frameworks of nanoscale, which are comprised of nanoparticles with the diameters of 70−120 nm. The Df of this fractal-like structure was about 1.51.

Witten and Sander[27] developed the mechanism of the aggregates' formation on a two-dimensional planar surface by introducing the concept of diffusion-limited aggregation (DLA). This model assumes that the particles originate far away from the developing immobile structure and perform a random walk in the surrounding space. The particle sticks to the existing structure once encounters it. This DLA model produces fractal-like structures with Df $= 1.71$. As mentioned above, PPE/DNA complexes with lower polymer ratio self-assembled into fractal-like structure with Df about 1.70, which was very close to that of the ideal system. However, when the polymer/DNA charge ratio was 1:1, the Df decreased to 1.51. The low Df values indicated a fast aggregation process where the probability of particle−particle sticking on collision was high.[28] Higher values of Df correspond to a slower aggregation process where the probability of sticking is low and thereby provides more compact aggregate structures. When the polymer/DNA charge ratio was adjusted to 1:1, the complex particles were neutral and resulted in a fast aggregation process.

As shown in Figure 3, the PPE/DNA complexes also self-assemble into fractal aggregates when the concentration of the PPEs and DNAs are high. Figure 3a shows the similar fractal-like structures in a perspective view. But actually the aggregation was composed of diffused particles, (inset in Figure 3a) which can be explained by the migration speed of the particles. The diameters of these particles vary from 0.4 to 1 μm, which were larger than those formed at lower concentrations. In the random walk process, the particles migrated more slowly than the globules of smaller size. To extend the random walk process, the deposited silicon substrate was put in a moisture atmosphere and dried slowly. Figure 3, parts b and c, shows the aggregate images of PPE1/DNA and PPE2/DNA, respectively, which are similar to the nanoscale aggregates at low concentrations. The fractal-like structures were composed of short helix wires with micrometer scale. The wires of PPE1/DNA complexes were 1−3 μm in diameter and several micrometers to several tens of micrometers in length, while the diameters of PPE2/DNA complexes were much larger at the same conditions. This is

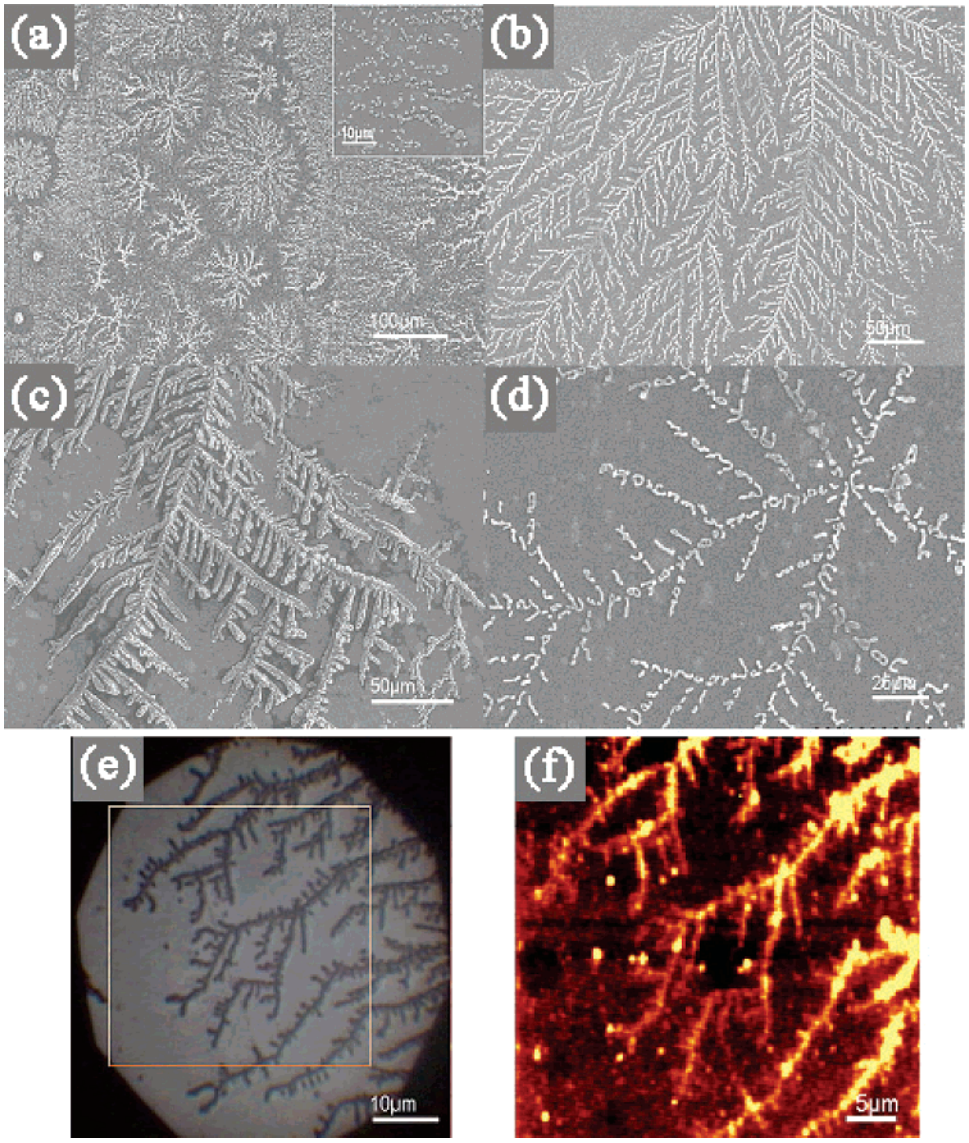

Figure 3. SEM images of (a) PPE1/dsDNA complexes with the DNA concentration of 5×10^{-7} M and PPE1/dsDNA charge ratio of 1:1; the inset is the magnified view that shows the aggregates are made up of dispersed particles; (b and c) PPE1, PPE2/dsDNA complexes with the DNA concentration of 5×10^{-7} M and PPEs/dsDNA charge ratio of 1:1; the silicon wafers were put in a moisture atmosphere for 2 h; (d) 40-mer PPE1/dsDNA complexes with the DNA concentration of 5×10^{-7} M and PPE1/dsDNA charge ratio of 1:1. (e) Optical image of the assembled aggregates of 25-mer dsDNA-fl (5×10^{-7} M) and PPE2 (PPE2/dsDNA charge ratio of 1:1). (f) CSLM image of the selected area.

mainly because PPE2 is shape-adaptable and can adapt to the range of the higher-order structures presented by the oligo-dsDNA, indicating that more conformational freedom can improve the contacts between the polymer and DNA. The Df of the two aggregates was 1.52 and 1.51, respectively, which was similar to the Df at low concentration, showing that the fractal dimension was independent of the concentration and the particle size but only related to the PPE/DNA charge ratio. Figure 3e shows the optical image of the fractal-like aggregates of 25-mer DNA-fl and PPE2 on a piece of cover glass. Figure 3f gives the confocal microscope image of the selected area with the emission of 488−588 nm detected and imaged, which is consistent with the optical image.

Oligo-dsDNA with 40 base pairs underwent a similar self-assembly process with the two PPEs. Figure 3d shows the aggregates were made up of twist microwires. As described above, these microwires were aggregates of large particles that underwent the DLA process and arranged in a fractal-like manner on substrates. Different from 25-mer oligo-dsDNA, the 40-mer dsDNA in these particles interacted more strongly so that they formed twist microwires when the solvent was evaporated.

Here we propose a schematic model to illustrate the self-assembly process (Figure 4). The interactions between the negatively charged oligo-DNA molecules and positively charged polymer, such as base stacking force, electrostatic interactions, van der Waals force, etc., cause the transformation of DNA structure from B to C and subsequently the formation of PPE/DNA complexes.[29] Deposited onto a two-dimensional substrate, the aggregates underwent DLA to form fractal structures. When the concentration is low, if the PPE/DNA charge ratio is high, in which case there is a slow particle collision, a nanoscale fractal structure with the Df of 1.70 grows. And the fractal dimension decreases to 1.51 when the particle collision process is rapid (the PPE/DNA charge ratio is near 1:1). When the concentration is high, due to the slow migration of the PPE/DNA complexes of larger scale, the fractal-like structure is made up of diffused particles. If the random walk process is extended

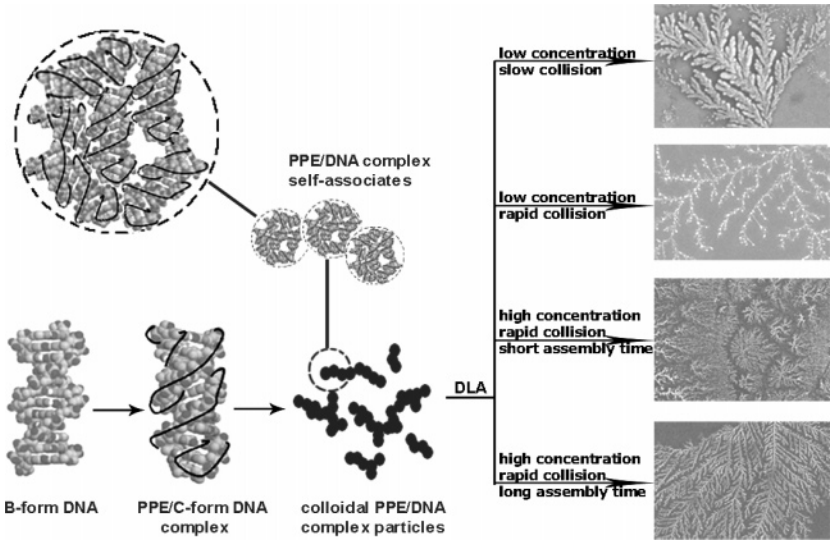

Figure 4. Proposed model of the fractal structural self-assembly process.

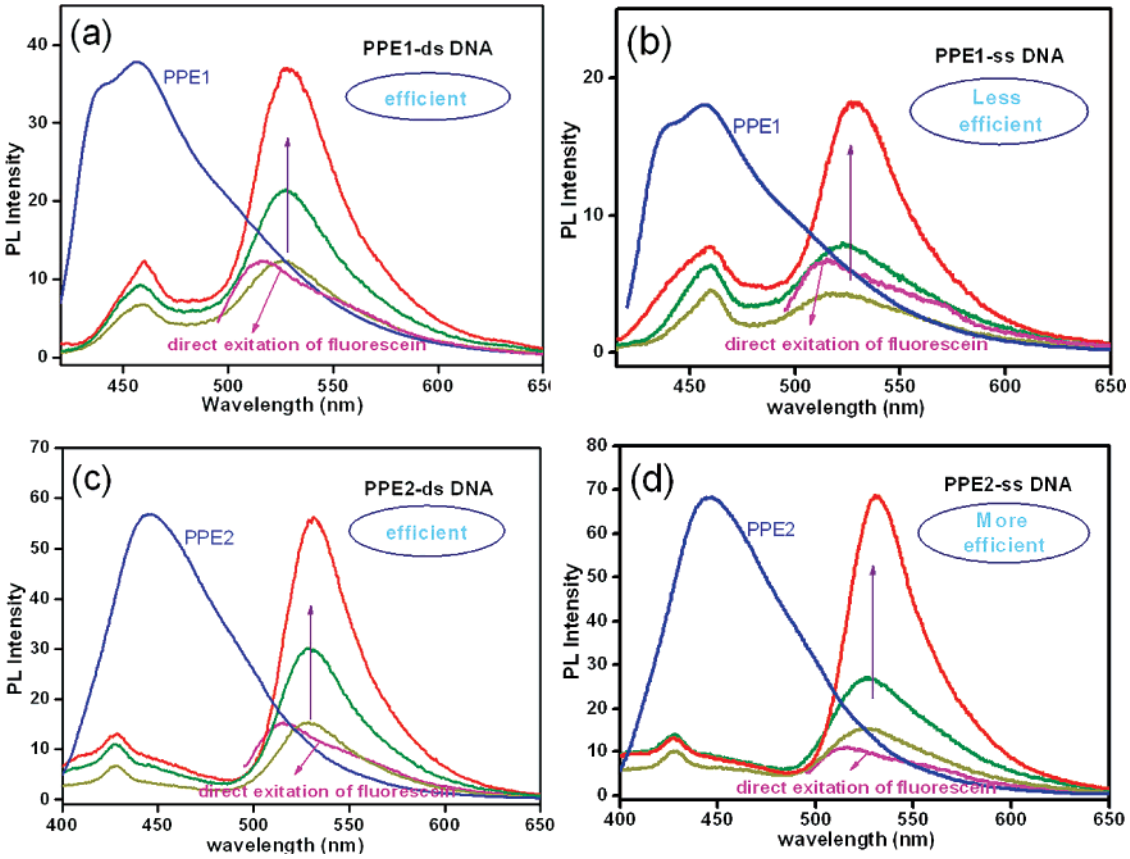

Figure 5. Emission spectra for mixtures of PPEs and DNAs-fl: the emission intensity of fluorescein increases with the addition of PPEs. [DNAs] = 1.25×10^{-7} M, [PPEs] = 5×10^{-6} to 5×10^{-5} M. The red line shows the FRET ratio reaches the maximum. The emission of PPEs (blue line) and direct excitation of fluorescein at its absorption maximum (480 nm, pink line) were recorded for comparison. (a) PPE1 and dsDNA-fl; (b) PPE1 and ssDNA-fl; (c) PPE2 and dsDNA-fl; (d) PPE2 and ssDNA-fl.

by increasing the assembly time, a highly ordered fractal structure of short wires can be obtained.

We have also found that the different FRET behavior between PPEs and DNA can be used to distinguish dsDNA from ssDNA. Recently, conjugated polymers have been widely developed as useful detecting tools in biosystems based on their electrochemical and optical properties upon complexation with target biomolecules.[30−34,37] Among the strategies, FRET is one of the most popular protocols due to its universality and sensitivity.[31−34] In our case, the good overlap between the emission spectra of the two PPEs and the absorption spectra of fluorescein ensures the FRET from PPEs to fluorescein. In FRET experiments, the excitation wavelength (400 nm for PPE1 and 385 nm for PPE2) was chosen where PPEs absorbs strongly and fluorescein shows negligible absorption. The FRET efficiency was evaluated by measuring the ratio of integrated acceptor to donor emission spectra.[33] As shown in Figure 5a, upon addition of PPE1 to a solution of dsDNA-fl, the emission intensity of the fluorescein dye increased intensively, but that of PPE1 increased much slower. This indicates that efficient FRET from PPE1 to dsDNA-fl occurs. Similar phenomena were observed in the FRET experiments of PPE1 to ss-DNA-fl, PPE2 to ds-DNA-fl, and

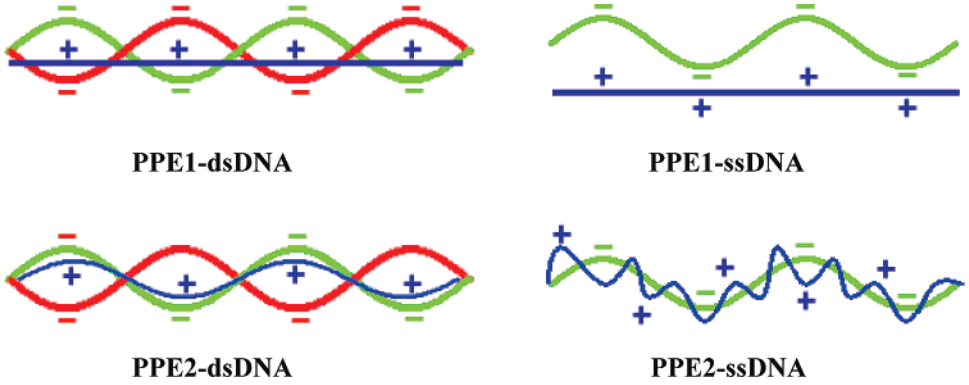

Figure 6. Schematic representation of the shape effect on the interactions between PPEs and DNAs.

PPE2 to ss-DNA-fl, which are shown in Figure 5b−d, respectively. Energy transfer was optimized by varying the charge ratio of PPEs to DNAs-fl. The results indicated that the maximal FRET ratio[34] of PPE1 to ds-DNA-fl (R_{P1-ds}), PPE1 to ss-DNA-fl (R_{P1-ss}), PPE2 to ds-DNA-fl (R_{P2-ds}), and PPE2 to ss-DNA-fl (R_{P2-ss}) are about 4.7, 2.5, 5.1, and 5.7, respectively.

As shown by Förster,[35] dipole−dipole interactions lead to long-range FRET and the energy transfer efficiency (E) is proportional to $1/r^6$, where r is the donor−acceptor distance, J is the spectra overlap integrals, and k is the orientation of transition moments.

$$E \propto \frac{1}{r^6} k^2 J(\lambda)$$

$$J(\lambda) = \int_0^\infty F_D(\lambda)\epsilon_A(\lambda)\lambda^4 \, d\lambda$$

In the systems of PPE1-dsDNA-fl and PPE1-ssDNA-fl, the spectra overlap integrals J are the same, as well as the transition moments k. Therefore, the difference in FRET efficiencies between PPE1 and DNAs will be most relevant to the distance (r) between the donor and acceptor. To understand the shape-influenced distance between the polymers and DNAs, the interactions are schematically shown in Figure 6. The persistent lengths of dsDNA and ssDNA are about 40 and 4 nm,[36] respectively; therefore, 25-mer dsDNA can be regarded as a linear rigid rod and 25-mer ssDNA should be considered as a semiflexible chain. In the systems of PPE1-dsDNA-fl and PPE1-ssDNA-fl, PPE1 has a linear polymer shape and can adapt neither the rigid rod like oligo-dsDNA nor semiflexible oligo-ssDNA. However, in comparison with ssDNA, the stronger electrostatic interactions of PPE1-dsDNA will result in a shorter distance between the donor and acceptor, which further influences the FRET ratio. ($R_{P1-ds} > R_{P1-ss}$).

In the systems of PPE2-dsDNA and PPE2-ssDNA, PPE2 has an adaptable shape and can adapt the conformations of dsDNA and ssDNA, which causes the more efficient FRET than those between PPE1 and DNAs.[37] More importantly, PPE2 and ssDNA are both semiflexible and can adapt to each other much more efficiently than PPE2 and rigid-rod dsDNA. The shape effect on the distance of PPE2 and DNAs is even larger than that caused by the electrostatic interactions. As a result, the FRET ratio of PPE2-ssDNA is higher than that of PPE2-dsDNA ($R_{P2-ds} < R_{P2-ss}$).

Signal amplification by the two PPEs provides a fluorescein emission that is over 4 times higher than that obtained by the direct excitation of the dye. Through the obviously different FRET behavior one can easily distinguish ds-DNA from ss-DNA.

Conclusions

In summary, we have demonstrated that the aggregates of self-assembly supramolecular conjugated polymers/DNA complexes can be controlled to give fractal-like structures. FRET and CD measurements showed the electrostatic interactions made the cationic polymer sufficiently close to oligo-DNA and then formed the DNA/polymer complex. Deposited onto a two-dimensional substrate, the complex underwent DLA and subsequently formed fractal structures. The two PPEs with a linear backbone and a nonlinear backbone showed different aggregation behavior, and their different FRET efficiencies could be used to distinguish dsDNA from ssDNA. The present work will provide a new detecting method for dsDNA and ssDNA and a novel molecular design concept for fabricating polymer supramolecular systems based on biological materials.

Acknowledgment. This work is supported by the National Nature Science Foundation of China (20531060, 10474101, 20418001, 20571078, 20421101, and 20473102) and Major State Basic Research Development Program (2005CB6623602 and 2006CB932100).

References and Notes

(1) Petka, W. A.; Harden, J. L.; McGrath, K. P.; Wirtz, D.; Tirrell, D. *Science* **1998**, *281*, 389.
(2) Chandler, D. *Nature* **2005**, *437*, 640.
(3) von Maltzahn, G.; Vauthey, S.; Santoso, S.; Zhang, S. *Langmuir* **2003**, *19*, 4332.
(4) Santoso, S.; Hwang, W.; Hartman, H.; Zhang, S. *Nano Lett.* **2002**, *2*, 687.
(5) Gosal, W. S.; Clark, A. H.; Pudney, P. D. A.; Ross-Murphy, S. B. *Langmuir* **2002**, *18*, 7174.
(6) Jung, J. H.; John, G.; Masuda, M.; Yoshida, K.; Shinkai, S.; Shimizu, T. *Langmuir* **2001**, *17*, 7229.
(7) Taira, S.; Du, Y.; Kodaka, M. *Biotechnol. Bioeng.* **2006**, *93*, 396.
(8) Vijayanathan, V.; Lyall, J.; Thomas, T.; Shirahata, A.; Thomas, T. J. *Biomacromolecules* **2005**, *6*, 1097.
(9) Kreiss, P.; Cameron, B.; Rangara, R.; Mailhe, P.; Aguerre-Charriol, O.; Airiau, M.; Scherman, D.; Crouzetand, J.; Pitard, B. *Nucleic Acids Res.* **1999**, *27*, 3792.
(10) Mitra, A.; Imae, T. *Biomacromolecules* **2004**, *5*, 69.
(11) Sarkar, S.; Lee, L. K.; Hart, S. L.; Hailes, H. C.; Levy, S. M.; Tabor, A.; Shamlou, P. A. *Biotechnol. Appl. Biochem.* **2005**, *41*, 127.
(12) Mao, C.; LaBean, T.; Reif, J. H.; Seeman, N. C. *Nature* **2000**, *407*, 493.
(13) Protozanova, E.; Macgregor, R. B., Jr. *Biochemistry* **1996**, *35*, 16638.
(14) Heeger, A. J. *Rev. Mod. Phys.* **2001**, *73*, 681.
(15) Fan, C.; Plaxco, K. W.; Heeger, A. J. *J. Am. Chem. Soc.* **2002**, *124*, 5642.
(16) Hoeben, F. J. M.; Jonkheijm, P.; Meijer, E. W.; Schenning, A. P. H. J. *Chem. Rev.* **2005**, *105*, 1491.
(17) Schenning, A. P. H. J.; Meijer, E. W. *Chem. Commun.* **2005**, 3245.
(18) Lam, J. W. Y.; Tang, B. Z. *Acc. Chem. Res.* **2005**, *38*, 745.
(19) Kim, J.; Swager, T. M. *Nature* **2001**, *411*, 1030.

(20) Jenekhe, S. A.; Chen, X. L. *Science* **1998**, *279*, 1903.
(21) Nelson, J. C.; Saven, J. G.; Moore, J. S.; Wolynes, P. G. *Science* **1997**, *277*, 1793.
(22) Tan C.; Pinto, M. R.; Kose, M. E.; Chiviriga, I.; Schanze, K. S. *Adv. Mater.* **2004**, *16*, 1208.
(23) Fan, Q. L.; Zhou, Y.; Lu, X. M.; Hou, X. Y.; Huang, W. *Macromolecules* **2005**, *38*, 2927.
(24) Zhang, Z.; Huang, W.; Tang, J.; Wang, E.; Dong, S. *Biophys. Chem.* **2002**, *97*, 7.
(25) Wang, Z. X.; Liu, D. J.; Dong, S. J. *Biophys. Chem.* **2000**, *87*, 179.
(26) Lomander, A.; Hwang, W.; Zhang, S. *Nano Lett.* **2005**, *5*, 1255.
(27) Witten, T.; Sander L. *Phys. Rev. Lett.* **1981**, *47*, 1400.
(28) Matsushita, M. *The Fractal Approach to Heterogeneous Chemistry*; John Wiley and Sons Ltd.: New York, 1989.
(29) Ghirlando, R.; Wachtel, E. J.; Arad, T.; Minsky, A. *Biochemistry* **1992**, *31*, 7110.
(30) Peng, H.; Soeller, C.; Travas-Sejdic, J. *Chem. Commun.* **2006**, 3735.
(31) Liu, B.; Bazan, G. C. *Chem. Mater.* **2004**, *16*, 4467.
(32) Lv, W.; Li, N.; Li, Y.; Li, Y.; Xia, A. *J. Am. Chem. Soc.* **2006**, *128*, 10281.
(33) Gaylord, B. S.; Heeger, A. J.; Bazan, G. C. *J. Am. Chem. Soc.* **2003**, *125*, 896.
(34) Gaylord, B. S.; Heeger, A. J.; Banzan, G. C. *Proc. Natl. Acad. Sci. U.S.A.* **2002**, *99*, 10954. The FRET ratio is defined as the integrated acceptor emission over the integrated emission of the donor.
(35) Förster, T. *Ann. Phys.* **1948**, *2*, 55.
(36) Grosberg, A. Y.; Khokhlov, A. R. *Statistical Physics of Macromolecules*; AIP Press: New York, 1994.
(37) Liu, B.; Wang, S.; Bazan, G. C.; Mikhailovsky, A. *J. Am. Chem. Soc.* **2003**, *125*, 13306.

BM070082K